



OPEN

# A branching bivariate weibull distribution model for evaluating exosomes in androgen-deprived agency in the presence of prostate cancer

M. Shanmugavalli<sup>1</sup>, K. Majella Jenvi Ignatia<sup>1</sup>, Mary Jiny D<sup>1</sup>, Raman Kumar<sup>2,3</sup>, Ashok Kumar Bishoyi<sup>4</sup>, S. Renuka Jyothi<sup>5</sup>, Harpreet Kaur Channi<sup>6</sup>, Abhijit Bhowmik<sup>7,8</sup> & Jasmina Lozanovic<sup>9</sup>✉

Castration-resistant prostate cancer (CRPC) poses a significant challenge in the medical field. The study developed a novel model, the branching bivariate Weibull distribution (BBWD), tailored to address CRPC and stems from the maximum likelihood estimation (MLE) function. It considers a medicinal biosystem aimed at transitioning androgen-dependent prostate cancer into an androgen-independent state. The BBWD model is designed to optimize the solution for bio variables pertinent to CRPC and evaluate various treatment techniques for androgen-dependent and androgen-independent behaviour. Through rigorous analysis, the kinetics of LINC01213 in androgen-deprived mediums are highlighted as promising, showing superior efficacy in castration compared to other techniques. The model utilizes the joint effect on the log-likelihood function (JELF) as a crucial analytical tool to assess the impact of LINC01213 in both normal and androgen-deprived medium. The results affirm the veracity of statements made within the medical field and support the notion that LINC01213 may serve as a novel therapeutic target for CRPC patients. The analysis underscores the pivotal role of exosomal LINC01213 in androgen-dependent prostate cancer, demonstrating its significance in treatment efficacy. The BBWD model highlighting the efficacy of LINC01213 in androgen-deprived mediums provides compelling evidence for its potential as a therapeutic target. This study corroborates existing medical hypotheses and offers detailed clarification and reports on treatment techniques for prostate cancer patients. Ultimately, it emphasizes the critical role of exosomal LINC01213 in addressing the challenges posed by androgen-dependent prostate cancer, offering a pathway toward more effective treatments.

**Keywords** Branching bivariate Weibull distribution (BBWD), Maximum likelihood estimation function (MLE), Log-likelihood function, Prostate cancer, Androgen deprived medium, Exosomes

## Abbreviations

BBWD                      Branching bivariate Weibull distribution  
JELF                        Joint effect on log-likelihood function

<sup>1</sup>Department of Mathematics, Saveetha School of Engineering, Saveetha Institute of Medical and Technical Sciences, SIMATS University, Chennai, Tamil Nadu 602105, India. <sup>2</sup>Department of Mechanical and Production Engineering, Guru Nanak Dev Engineering College, Ludhiana, Punjab 141006, India. <sup>3</sup>Jadara Research Center, Jadara University, Irbid 21110, Jordan. <sup>4</sup>Department of Microbiology, Marwadi University Research Center, Faculty of Science, Marwadi University, Rajkot, Gujarat 360003, India. <sup>5</sup>Department of Biotechnology and Genetics, School of Sciences, JAIN (Deemed to be University), Bangalore, Karnataka, India. <sup>6</sup>Department of Electrical Engineering, Chandigarh University, Mohali 140413, India. <sup>7</sup>Department of Mechanical Engineering, Graphic Era (Deemed to be University), Clement Town, Dehradun 248002, India. <sup>8</sup>Centre for Research Impact and Outcome, Chitkara University Institute of Engineering and Technology, Chitkara University, Rajpura, Punjab 140401, India. <sup>9</sup>Department of Engineering, FH Campus Wien - University of Applied Sciences, Favoritenstraße 226, 1100 Vienna, Austria. ✉email: jasmina.lozanovic@fh-campuswien.ac.at

MLE	Maximum likelihood estimation
CRPC	Castration resistant and prostate cancer
LINC01213	Long intergenic non-coding RNA1213
LNcaP	Lymph node carcinoma of the prostate
Si-LINC01213	Sacroiliac long intergenic non-coding RNA1213
PC-3	Human prostate cancer cell line
AR	Androgen receptor
PSA	Prostate specific antigen
MRI	Magnetic resonance imaging
DNA	Deoxyribonucleic acid
PSMA	Prostate specific membrane antigen
NOTCH3	Neurogenic locus notch homolog protein 3
ADPC	Androgen dependent prostate cancer
AIPC	Androgen independent prostate cancer
RNA	Ribonucleic acid
MicroRNA	Micro ribonucleic acid
lncRNA	Long non-coding RNA
circRNA	Circular RNA

Prostate cancer is the most prevalent cause of cancer-related fatalities in Western countries, primarily affecting men in their middle age between 45 and 60 years of age<sup>1</sup>. There are variations in prostate cancer epidemiology since many men are identified with the disease using methods such as digital rectal examination, PSA testing, magnetic resonance imaging (MRI), or prostate biopsy and analysis<sup>2</sup>. Prostate cancer risk factors include age, weight, race, family history, and other environmental variables. Because of variations in genetics and epidemiology, prostate cancer is a diverse illness with many contributing factors. The interaction of genetics, environment, and social factors results in estimates of the prostate cancer survival rate that are racist.

Prostate cancer and genetics are known to be related. The genetic predisposition to prostate cancer and hereditary prostate cancer has been the subject of years of investigation. One of the biggest genetic risk factors for prostate cancer is family inheritance. Twin studies and epidemiological research have shown the importance of hereditary prostate cancer<sup>3</sup>. Numerous investigators have examined the potential contribution of genetic diversity to androgen production, metabolism, and function<sup>4,5</sup>. Chromosome rearrangements are among the molecular mechanisms that genomics research has linked to the development of some cancers<sup>2</sup>.

Mutations in specific genes often lead to cancer. Prostate cancer susceptibility genes may include those related to the androgen pathway and testosterone metabolism. Prostate epithelial cells and prostate cancer cells develop only in the presence of testosterone and the androgen receptor signalling pathway<sup>6</sup>. By focusing on specific genetic defects and finding cancer biomarkers, prostate cancer can be appropriately treated. Among the biomarkers used for targeted therapy are DNA tumour, general, and DNA biomarkers<sup>7</sup>.

In prostate cancer, the terms “androgen sensitivity” and “androgen insensitivity” relate to the degree of testosterone stimulation and available treatment options. Prostate cancer can be treated with a variety of techniques, including surgery, hormone therapy, radiation therapy, active surveillance, and cryotherapy. Treatment choices are contingent upon the type of tumour, PSA level, grade, stage, and likelihood of recurrence. Radiation therapy, for example, is used in conjunction with radical prostatectomy. This surgical procedure involves the removal of the prostate and surrounding tissues to treat low-risk prostate cancer<sup>8</sup>. Treatment recommendations for cancers that have returned and spread outside the prostate include hormonal therapy, also referred to as androgen-deprivation therapy<sup>1</sup>.

The most compelling theory regarding exosomes is that they are vesicular carriers that control gene expression and resemble viruses<sup>9</sup>. The result supports creating a new PSMA-based exosome capture technology platform that can effectively tell the difference between exosomes made by prostate tumours and those connected to healthy tissue. The antiviral and NOTCH3 pathways may work together as biomarkers and therapeutic targets to treat antibiotic resistance caused by stromal cells<sup>10</sup>. Blood can act as a carrier in cell–cell and organ communication since it is a physiological fluid that the body uses to circulate exosomes<sup>11</sup>.

People with CRPC have a hard time getting treatment because the disease changes from being androgen-dependent to androgen-independent. This makes standard androgen-deprivation therapies (ADT) less effective. Current therapies for CRPC are far from ideal, and effective predictive models that would capture the intricate biochemical interactions involved are sorely needed.

Recent studies have highlighted the importance of exosomes, small vesicles secreted by cells as carriers of regulatory molecules, especially RNAs. Among these, long non-coding RNAs (lncRNAs) have gained attention for their role in cancer progression. Exosomal lncRNAs, such as lncRNA-p21, have shown potential as diagnostic markers in prostate cancer, and others, like PCGEM1 and PRNCR1, are linked to androgen receptor signaling<sup>12</sup>. LINC01213, a less-explored lncRNA, has been implicated in cancer-related pathways and may play a role in the transition from androgen-dependent to androgen-independent states. This study examines the role of LINC01213 in exosomes in the progression of CRPC, aiming to elucidate its impact on RNA-mediated cell communication and resistance mechanisms<sup>13</sup>.

A new player in the list of molecular modulators of androgen dependency is the non-coding RNA LINC01213, which has emerged as a potential therapeutic target for manipulating the androgen dependency of prostate cancer cells. However, traditional survival models can't be used to figure out how exosomal interactions affect the progression of prostate cancer when there isn't enough androgen. Thus, the problem is designing a statistically advanced model that captures these complex interactions and provides insight into how LINC01213 is effective in androgen-deprived environments. So, the following research objectives are laid out.

- Development of a BBWD model to address the complex dynamics of the survival of CRPC cells. It could incorporate both androgen-dependent and androgen-independent behaviors.
- Exploring effects of exosomal LINC01213 on the behaviour of prostate cancer cells in a regular and androgen-deprived environment with the aid of BBWD combined analysis tool: application of JELF.
- LINC01213 target therapeutic interventions on CRPC Patients: To identify and test LINC01213 as a target therapeutic intervention and compare its efficacy in supporting the survival of androgen-independent cells with another therapy.
- Statistical validation for individualized prostate cancer treatment plans to develop personalized prostate cancer treatment plans that enhance beneficial therapeutic results by examining tumours' behaviours and sensitivity to androgen deprivation.

This is the first study to introduce a BBWD model as a new method for analyzing CRPC. At a time when critical gaps exist within existing statistical toolkits for assessing efficacy in treatment due to complex biochemical interactions, the focus on exosomal LINC01213 offers rich insights into a new, potentially transformative therapeutic target that may further enhance treatment options for CRPC patients resistant to conventional therapies.

Numerous statistical models have been employed to investigate the relationship between biochemical markers and disease progression in CRPC. Among them, the BBWD stands out because it can effectively illustrate how two related events, such as PSA levels and disease progression, influence each other.

The FGM Bivariate Weibull model is effective when the relationship between two variables is weak. But CRPC often shows stronger and more complex connections, which this model cannot fully capture<sup>14</sup>. The bivariate inverse Weibull model is suitable for specific medical data with unusual risk patterns. However, CRPC usually shows steady (monotonic) risk over time, so this model doesn't fit well. Multi-state Weibull models are useful for tracking changes between disease stages. While helpful, they don't focus on the relationship between markers and survival time, which is key in CRPC research<sup>15</sup>.

In contrast, BBWD can model how one event can affect another, making it ideal for CRPC. It better reflects the real interactions between biomarkers and patient outcomes. In short, while other models give helpful information, BBWD is more powerful and flexible for studying the complex biology of CRPC.

The study makes a methodological contribution to biostatistics by demonstrating how more advanced survival models can be applied to medical and oncological research. Their findings also help advance personalized medicine approaches with a strategy for customizing treatment regimens that may benefit patients and minimize side effects. This study supports pending hypotheses in cancer biology through rigorous analysis and validation, thus paving the way for further studies on the role of other biomarkers and molecular pathways in managing CRPC.

The study presents a novel distribution that provides significant insights into the treatment terrain for CRPC. It shows how well LINC01213 works when there aren't enough androgens, highlighting the vital part that exosomal LINC01213 plays in fighting the problems that come with androgen-dependent prostate cancer. Ultimately, it paves the way for enhanced treatment strategies.

### Novelty and objective of the study

Using exosomal LINC01213 in conjunction with the BBWD yields a novel and enhanced approach to modeling the growth of CRPC. LINC01213, carried within tumour-derived exosomes, plays a key role in the shift from androgen-dependent to androgen-independent prostate cancer by activating the Wnt/ $\beta$ -catenin signalling pathway, a hallmark mechanism in CRPC progression<sup>16</sup>.

Due to the limitations of traditional models outlined in the previous section, the BBWD model was introduced as a more suitable alternative for capturing the complex interdependencies in CRPC progression. On the other hand, the BBWD model can handle strong, branching dependencies between two time-to-event variables that are connected, like exosomal LINC01213 levels and time to disease progression. This branching structure reflects how an increase in LINC01213 expression can directly impact both the timing and likelihood of CRPC progression.

What makes this integration novel is the direct linkage between a molecular mechanism and a high-resolution statistical framework. By embedding exosomal LINC01213 into the BBWD model, this study captures the stochastic nature of CRPC progression more accurately than any previous models.

This integration offers a dual-level advantage: biological insight, as it helps reveal how exosomal LINC01213 drives the molecular cascade in CRPC. Statistical modeling: It tracks how fluctuations in this biomarker influence the timing and likelihood of disease milestones. As a result, the proposed model not only improves predictive accuracy but also enables the identification of potential therapeutic windows, paving the way for personalised treatment strategies targeting exosomal RNA pathways in CRPC.

## Methods

### Introduction for the mathematical part

The Weibull distribution is the most commonly employed when modelling survival and failure time data. It has various applications, and specialists have examined all of its properties. Since the 1970s, several extensions to the Weibull distribution have been proposed, which can be used to describe complex lifetime data beyond the scope of the original Weibull. They are often used in stability and durability analysis. There are multiple Weibull-related distributions beyond the two- and three-parameter typical Weibull distributions found in the literature on statistics and stability. Lu and Bhattacharya have defined the bivariate Weibull distribution in detail and created a multivariate survival function for the Weibull distribution<sup>17</sup>.

In 1999, Richard A. Johnson et al. discussed the strengths and weaknesses of various bivariate distributions, including the exponential distribution, the normal distribution, the log-normal distribution, the inverse Gaussian distribution, the SBB distribution, and the normal-lognormal distribution<sup>18</sup>. Finally, they selected the proposed bivariate distribution, specifically the bivariate Weibull distribution, for further discussion.

A non-linear transformation in Gaussian variables has been introduced to generalise the covariance matrix into a non-linear covariance matrix<sup>19</sup>. That portfolio distribution is illustrated in detail for the multivariate Weibull distribution. For survival analysis, a positive stable frailty distribution was employed, allowing for both parametric and non-parametric inference of censored data, which resulted in ordered failure time data<sup>20</sup>. The flexible baseline hazard model, considering the gamma frailty model, was correlated with a standard Weibull model<sup>21</sup>. It has been proposed that a continuous bivariate Weibull distribution may be successfully employed by eliminating the singular component if the data set contains no ties and the marginals have a heavy-tailed distribution<sup>22,23</sup>.

In wind speed and direction measurements, the Weibull probability distribution function has been proposed as a model to determine the relevant monthly frequency distributions<sup>24</sup>. The multivariate Marshall-Olkin Weibull distribution gave the best singular distribution with non-zero probability, even if the sample size increased<sup>23</sup>. According to Kundu and Gupta, a generalised Marshall-Olkin distribution can be described using a flexible five-parameter bivariate distribution<sup>25</sup>. Some interesting examples are the lengths of people's lives in genetic epidemiology, dental implants for patients, and the births of monozygotic and dizygotic twins, where the unknown and random genetic behaviour of patients follows the known frailty distribution. These circumstances stimulated Hanagal to develop a bivariate Weibull regression model<sup>26</sup>.

Maximum likelihood estimation is a practical approach in statistical modeling strategies for nonlinear modeling. The need for its hazard function nonetheless restricts its monotonic application regardless of the values of its parameters, even though it may be increasing or decreasing. This makes these kinds of distributions useful in the medical profession for analyzing the validity of illnesses that the medical field identifies. In cases where the disease progresses to the point where mortality peaks after a certain amount of time and then gradually falls, this may not be the best course of action. Renal density and failure density functions were used in the comparison of cesarean sections and vaginal deliveries to assess oxytocin release in the nervous system<sup>27</sup>.

A changed version of the Weibull distribution was used to talk about the conclusion that prolactin and premenopausal cases are much less common in postmenopausal instances when it comes to serum prolactin levels and breast cancer risk<sup>28</sup>. The stochastic gamma process and the Weibull distribution have been used to explain growth hormone-related difficulties<sup>29,30</sup>. In research on the curability of breast cancer, it was found that the peak mortality rate occurred approximately three years after diagnosis. The log-logistic distribution provides a parametric form for such a hazard.

Although the log-logistic and log-normal distributions are similar, the log-logistic distribution is more suitable for analyzing survival data. This results from its improved mathematical tractability when handling the frequently occurring censored observations of such data. The value of the survivor function at the moment of censoring is the contribution a right-censored observation makes to the likelihood. For the log-logistic distribution, this may be assessed explicitly; however, for the log-normal. Additionally, it will be demonstrated that the hazard functions for various samples in this regression model are not proportional.

The ability of these semi-parametric models to evaluate treatment disparities, risk factors, and prognostic factors has sparked interest in examining more specific life history details. For instance, one might want to examine the bivariate distribution of two time variables or incorporate the timing of one event into a regression analysis of another event in life. A general framework for modelling life histories in terms of counting processes has been developed, offering a structured approach to analyze such data.

The works by Majella K. and Lakshmi S. collectively focus on the application of mathematical and stochastic modelling techniques to understand and quantify hormonal dynamics, particularly estrogen and its physiological impacts, encompassing areas such as hormone secretion, bone density regulation, and the effects of hormone therapy in clinical contexts<sup>31–35</sup>. Ultimately, the study develops a proportional hazards regression model that incorporates both random and fixed components.

Building upon this foundation of hormone-focused mathematical modeling, the present study advances to a broader analytical framework involving survival analysis and hazard function modeling.

### Multifunction derivation from bivariate Weibull distribution

The Joint Survival function was developed to model the combined survival behavior of two variables which includes the two arbitrary failure rate functions,  $h_1(x)$  and  $h_2(y)$  along with the related cumulative failure rate  $H_1(x)$  and  $H_2(y)$  on  $[0, \infty)$

$$\bar{F}(x, y/s) = \exp \{ -[H_1(x) + H_2(y)]^\gamma s \}$$

where the conditional link between  $x$  and  $y$  is measured by  $\gamma$ .

With reference to this function, let us assume that there exist two joint survival functions, namely  $\bar{F}_1(x, y/s)$  and  $\bar{F}_2(y, z/s)$  as

$$\begin{aligned}\bar{F}_1(x, y/s) &= \exp \{ -[H_1(x) + H_2(y)]^\gamma s \} \\ \bar{F}_2(y, z/s) &= \exp \{ -[H_3(y) + H_4(z)]^\gamma s \}\end{aligned}$$

where  $H_1(x)$ ,  $H_2(y)$ ,  $H_3(y)$ ,  $H_4(z)$  are cumulative failure rates on  $[0, \infty)$ .

Also, where the conditional link between  $x$  and  $y$  is measured by  $\gamma$  in  $\bar{F}_1$ , and where the conditional link between  $y$  and  $z$  is measured by  $\gamma$  in  $\bar{F}_2$ .

Next, assuming that the Laplace transform of the series  $S$  exists on  $[0, \infty)$ , Lu and Bhattacharya calculated the bivariate survival function  $\bar{F}(x, y/s)$  from the marginals  $\bar{F}_x$  and  $\bar{F}_y$  and discovered that it is strictly decreasing. The following is the generated Bivariate Weibull Distribution:

$$\bar{F}(x, y) = \exp \left\{ - \left[ \left( \frac{x}{\lambda_1} \right)^{\frac{\gamma_1}{\alpha}} + \left( \frac{y}{\lambda_2} \right)^{\frac{\gamma_2}{\alpha}} \right]^\alpha \right\}$$

where  $0 < \alpha \leq 1, 0 < \lambda_1, \lambda_2 < \infty, 0 < \gamma_1, \gamma_2 < \infty$ .

On repeating the same procedure, we can extend this to

$$\bar{F}_1(x, y) = \exp \left\{ - \left[ \left( \frac{x}{\lambda_1} \right)^{\frac{\gamma_1}{\alpha}} + \left( \frac{y}{\lambda_2} \right)^{\frac{\gamma_2}{\alpha}} \right]^\alpha \right\}$$

$$\bar{F}_2(x, y) = \exp \left\{ - \left[ \left( \frac{y}{\epsilon_1} \right)^{\frac{\theta_1}{\beta}} + \left( \frac{z}{\epsilon_2} \right)^{\frac{\theta_2}{\beta}} \right]^\beta \right\}$$

where  $0 < \alpha, \beta \leq 1, 0 < \lambda_1, \lambda_2 < \infty, 0 < \gamma_1, \gamma_2 < \infty, 0 < \epsilon_1, \epsilon_2 < \infty$ , and  $0 < \theta_1, \theta_2 < \infty$ .

These bivariate distributions can be expanded to include more than two variables and up to  $n$  variables by proceeding with the steps.

Consequently, they created a multivariate survival function of the Weibull distribution, which is

$$s(x_1, x_2, x_3, \dots, x_n) = \exp \left\{ - \left[ \left( \frac{x_1}{\lambda_1} \right)^{\frac{\gamma_1}{\alpha}} + \left( \frac{x_2}{\lambda_2} \right)^{\frac{\gamma_2}{\alpha}} + \dots + \left( \frac{x_n}{\lambda_n} \right)^{\frac{\gamma_n}{\alpha}} \right]^\alpha \right\}$$

As per the previous procedure, here we can also construct the two different multivariate survivals of the Weibull distribution as follows:

$$s_1(x_1, x_2, x_3, \dots, x_n) = \exp \left\{ - \left[ \left( \frac{x_1}{\lambda_1} \right)^{\frac{\gamma_1}{\alpha}} + \left( \frac{x_2}{\lambda_2} \right)^{\frac{\gamma_2}{\alpha}} + \dots + \left( \frac{x_n}{\lambda_n} \right)^{\frac{\gamma_n}{\alpha}} \right]^\alpha \right\}$$

and

$$s_2(y_1, y_2, y_3, \dots, y_n) = \exp \left\{ - \left[ \left( \frac{y_1}{\epsilon_1} \right)^{\frac{\theta_1}{\beta}} + \left( \frac{y_2}{\epsilon_2} \right)^{\frac{\theta_2}{\beta}} + \dots + \left( \frac{y_n}{\epsilon_n} \right)^{\frac{\theta_n}{\beta}} \right]^\beta \right\}$$

with  $0 < \alpha, \beta \leq 1, 0 < \lambda_1, \lambda_2, \dots, \lambda_n < \infty, 0 < \gamma_1, \gamma_2, \dots, \gamma_n < \infty, 0 < \epsilon_1, \epsilon_2, \dots, \epsilon_n < \infty$ , and  $0 < \theta_1, \theta_2, \dots, \theta_n < \infty$ .

Finding the multivariate probability density function

$$f(x_1, x_2, \dots, x_n) = (-1)^n \frac{\partial^n s(x_1, x_2, \dots, x_n)}{\partial x_1 \partial x_2 \dots \partial x_n} \quad (1)$$

Using (1), The probability density function was derived to provide mathematical description of the distribution.

$$f(x_1, x_2, x_3, \dots, x_n) = \left( \frac{-1}{\alpha} \right)^n \exp \left\{ - \left[ \left( \frac{x_1}{\lambda_1} \right)^{\frac{\gamma_1}{\alpha}} + \left( \frac{x_2}{\lambda_2} \right)^{\frac{\gamma_2}{\alpha}} + \dots + \left( \frac{x_n}{\lambda_n} \right)^{\frac{\gamma_n}{\alpha}} \right]^\alpha \right\} \\ \left[ \left( \frac{\gamma_1}{\lambda_1} \right) \left( \frac{\gamma_2}{\lambda_2} \right) \dots \left( \frac{\gamma_n}{\lambda_n} \right) \right] \left[ \left( \frac{x_1}{\lambda_1} \right)^{\frac{\gamma_1}{\alpha} - 1} + \left( \frac{x_2}{\lambda_2} \right)^{\frac{\gamma_2}{\alpha} - 1} + \dots + \left( \frac{x_n}{\lambda_n} \right)^{\frac{\gamma_n}{\alpha} - 1} \right] \\ \sum_{i=1}^{P(n)} (-1)^{k_i} P_S(n, j) \prod_{j=1}^{k_i} \alpha^{n_j} \left[ \left( \frac{x_1}{\lambda_1} \right)^{\frac{\gamma_1}{\alpha}} + \left( \frac{x_2}{\lambda_2} \right)^{\frac{\gamma_2}{\alpha}} + \dots + \left( \frac{x_n}{\lambda_n} \right)^{\frac{\gamma_n}{\alpha}} \right]^{k_i \alpha - n}$$

where  $k_i$  is the number of summands of the  $i$ th partition of  $n$  such that  $n_1 + n_2 + \dots + n_{k_i} = n, n_1 \geq n_2 \geq \dots \geq n_{k_i} > 0, 1 \leq k_i \leq n$

Furthermore, we are going to focus on the bivariate probability density function and its efficacy. As we are following only a bivariate probability density function, (1) becomes

$$f(x_1, x_2) = (-1)^2 \frac{\partial^2 s(x_1, x_2)}{\partial x_1 \partial x_2}$$

So, we can infer that,

$$\frac{\partial s}{\partial x_2} = - \left( \frac{\gamma_2}{\lambda_2} \right) \exp \left\{ - \left[ \left( \frac{x_1}{\lambda_1} \right)^{\frac{\gamma_1}{\alpha}} + \left( \frac{x_2}{\lambda_2} \right)^{\frac{\gamma_2}{\alpha}} \right]^\alpha \right\} \left( \frac{x_2}{\lambda_2} \right)^{\frac{\gamma_2}{\alpha} - 1} \left[ \left( \frac{x_1}{\lambda_1} \right)^{\frac{\gamma_1}{\alpha}} + \left( \frac{x_2}{\lambda_2} \right)^{\frac{\gamma_2}{\alpha}} \right]^{\alpha - 1}$$

As a result, we derive

$$f(x_1, x_2) = \frac{\partial^2 s}{\partial x_1 \partial x_2} = \left( \frac{\gamma_1 \gamma_2}{\alpha x_1 x_2} \right) \exp \left\{ - \left[ \left( \frac{x_1}{\lambda_1} \right)^{\frac{\gamma_1}{\alpha}} + \left( \frac{x_2}{\lambda_2} \right)^{\frac{\gamma_2}{\alpha}} \right]^\alpha \right\} \left( \frac{x_1}{\lambda_1} \right)^{\frac{\gamma_1}{\alpha}} \left( \frac{x_2}{\lambda_2} \right)^{\frac{\gamma_2}{\alpha}} \\ \times \left[ \left( \frac{x_1}{\lambda_1} \right)^{\frac{\gamma_1}{\alpha}} + \left( \frac{x_2}{\lambda_2} \right)^{\frac{\gamma_2}{\alpha}} \right]^{\alpha-2} \left\{ 1 + \alpha \left( -1 + \left[ \left( \frac{x_1}{\lambda_1} \right)^{\frac{\gamma_1}{\alpha}} + \left( \frac{x_2}{\lambda_2} \right)^{\frac{\gamma_2}{\alpha}} \right]^\alpha \right) \right\}$$

This is referred to as the probability density function of a bivariate distribution. To estimate the parameters involved in this bivariate distribution, the Maximum Likelihood Estimation (MLE) method is employed.

### Maximum likelihood estimation (MLE) parameter

Maximum Likelihood Estimation (MLE) is used to find model parameter values. The estimated parameter value should reflect the maximum likelihood of the data we collected. Optimizing a likelihood function makes observed data more likely under the postulates of a statistical model. So, the log-likelihood function for the defined bivariate Weibull distribution  $f(x_1, x_2)$  has been derived as.

For a bivariate Weibull distribution, the MLE approach involves the following:

Let  $(x_1, y_1), (x_2, y_2), \dots, (x_n, y_n)$  be a random sample from a bivariate Weibull distribution characterized by parameter vector  $\theta = (\alpha_1, \beta_1, \alpha_2, \beta_2, \lambda)$ , where:

- $\alpha_1, \alpha_2$  are shape parameters,
- $\beta_1, \beta_2$  are scale parameters,
- $\lambda$  is the dependence parameter (in some models, such as the Marshall-Olkin or other copula-based forms).

The joint probability density function (pdf)  $f(x, y; \theta)$  is used to form the likelihood function:

$$L(\theta) = \prod_{i=1}^n f(x_i, y_i; \theta)$$

To simplify computation, the log-likelihood function is used:

$$L(x) = \ln L(\theta) = \sum_{i=1}^n \ln f(x_i, y_i; \theta)$$

The MLEs of the parameters are the values of  $\theta$  that maximize this log-likelihood function. So, log-likelihood function for the defined bivariate weibull distribution  $f(x_1, x_2)$  has been derived as

$$L(x) = \sum_{i=1}^n \ln f(x_1, x_2) = \sum_{i=1}^n \ln \left( \frac{\gamma_1 \gamma_2}{\alpha x_1 x_2} \right) - \sum_{i=1}^n \left[ \left( \frac{x_{1i}}{\lambda_1} \right)^{\frac{\gamma_1}{\alpha}} + \left( \frac{x_{2i}}{\lambda_2} \right)^{\frac{\gamma_2}{\alpha}} \right]^\alpha \\ + \sum_{i=1}^n \frac{\gamma_1}{\alpha} \ln \left( \frac{x_{1i}}{\lambda_1} \right) + \sum_{i=1}^n \frac{\gamma_2}{\alpha} \ln \left( \frac{x_{2i}}{\lambda_2} \right) + \sum_{i=1}^n (\alpha - 2) \ln \left[ \left( \frac{x_{1i}}{\lambda_1} \right)^{\frac{\gamma_1}{\alpha}} + \left( \frac{x_{2i}}{\lambda_2} \right)^{\frac{\gamma_2}{\alpha}} \right]^\alpha \\ + \sum_{i=1}^n \ln \left\{ 1 + \alpha \left( -1 + \left[ \left( \frac{x_{1i}}{\lambda_1} \right)^{\frac{\gamma_1}{\alpha}} + \left( \frac{x_{2i}}{\lambda_2} \right)^{\frac{\gamma_2}{\alpha}} \right]^\alpha \right) \right\}$$

### Joint effect on log-likelihood function (JELF)

Similarly, for the bivariate Weibull distribution, the joint effect on the log-likelihood function has been determined and demonstrated as



$$\begin{aligned}
& \sum_{k_1=1}^n \ln f_1(x_1, x_2) + \sum_{k_2=1}^m \ln f_2(y_1, y_2) = \sum_{i=1}^n \ln \left( \frac{\gamma_1 \gamma_2}{\alpha x_1 x_2} \right) + \sum_{i=1}^n \left[ \left( \frac{x_{1i}}{\lambda_1} \right)^{\frac{\gamma_1}{\alpha}} + \left( \frac{x_{2i}}{\lambda_2} \right)^{\frac{\gamma_2}{\alpha}} \right]^\alpha \\
& + \sum_{i=1}^n \frac{\gamma_1}{\alpha} \ln \left( \frac{x_{1i}}{\lambda_1} \right) + \sum_{i=1}^n \frac{\gamma_2}{\alpha} \ln \left( \frac{x_{2i}}{\lambda_2} \right) \\
& + \sum_{i=1}^n (\alpha - 2) \ln \left[ \left( \frac{x_{1i}}{\lambda_1} \right)^{\frac{\gamma_1}{\alpha}} + \left( \frac{x_{2i}}{\lambda_2} \right)^{\frac{\gamma_2}{\alpha}} \right]^\alpha \\
& + \sum_{i=1}^n \ln \left\{ 1 + \alpha \left( -1 + \left[ \left( \frac{x_{1i}}{\lambda_1} \right)^{\frac{\gamma_1}{\alpha}} + \left( \frac{x_{2i}}{\lambda_2} \right)^{\frac{\gamma_2}{\alpha}} \right]^\alpha \right) \right\} \\
& + \sum_{i=1}^m \ln \left( \frac{\theta_1 \theta_2}{\beta y_1 y_2} \right) - \sum_{i=1}^m \left[ \left( \frac{y_{1i}}{\epsilon_1} \right)^{\frac{\theta_1}{\beta}} + \left( \frac{y_{2i}}{\epsilon_2} \right)^{\frac{\theta_2}{\beta}} \right]^\beta \\
& + \sum_{i=1}^m \frac{\theta_1}{\beta} \ln \left( \frac{y_{1i}}{\epsilon_1} \right) + \sum_{i=1}^m \frac{\theta_2}{\beta} \ln \left( \frac{y_{2i}}{\epsilon_2} \right) \\
& + \sum_{i=1}^m (\beta - 2) \ln \left[ \left( \frac{y_{1i}}{\epsilon_1} \right)^{\frac{\theta_1}{\beta}} + \left( \frac{y_{2i}}{\epsilon_2} \right)^{\frac{\theta_2}{\beta}} \right]^\beta \\
& + \sum_{i=1}^m \ln \left\{ 1 + \beta \left( -1 + \left[ \left( \frac{y_{1i}}{\epsilon_1} \right)^{\frac{\theta_1}{\beta}} + \left( \frac{y_{2i}}{\epsilon_2} \right)^{\frac{\theta_2}{\beta}} \right]^\beta \right) \right\}
\end{aligned}$$

Overall, it is a foundational concept in statistical inference and modelling across various scientific and engineering fields. Accordingly, the author adopts this approach to evaluate the combined influence of parameters, ensuring the robustness and reliability of the proposed model.

### Collective observation of joint effect on log-likelihood function on three functions

We can provide the joint effect log-likelihood function (JELF) for three functions collectively, as follows:

$$JELF = \sum_{k_1=1}^n \ln f_1(x_1, x_2) + \sum_{k_2=1}^m \ln f_2(y_1, y_2) + \sum_{k_3=1}^p \ln f_3(z_1, z_2) \quad (2)$$

In the same way, the same can be derived for a finite number of observations fixed over the Weibull distributions as.

$$\sum_{k_1=1}^n \ln f_1(x_1, x_2) + \sum_{k_2=1}^m \ln f_2(y_1, y_2) + \sum_{k_3=1}^p \ln f_3(z_1, z_2) + \cdots + \sum_{k_N=1}^w \ln f_N(\phi_1, \phi_2)$$

Density estimation is the main problem in estimating the probability distribution with a sample of observations from the given phenomenon. Though many techniques are used to resolve density estimation, a beneficial function that can be used is the maximum likelihood function (MLE).

### Mathematical parameter estimation and validation

The proposed model parameters were estimated using time-to-event data sourced from Guo et al.<sup>16</sup>, which provides empirical measurements of exosomal LINC01213 expression and clinical progression events in CRPC.

#### Parameter estimation using statistical inference

In the absence of primary experimental data, the BBWD model parameters, specifically the shape parameters  $\gamma_1, \gamma_2$ , scale parameters  $\lambda_1, \lambda_2$ , and the branching dependence parameter  $\alpha$  were inferred by fitting the joint probability distribution to the empirical survival and biomarker datasets.

This involved maximizing the joint likelihood function  $L(x)$  constructed from the bivariate time-to-event observations  $\left\{ \left( t_1^{(i)}, t_2^{(i)} \right) \right\}_{i=1}^n$ . Numerical optimization techniques were employed to identify parameter estimates  $\theta = (\gamma_1, \gamma_2, \lambda_1, \lambda_2, \alpha)$  that best describes the stochastic dependence structure between exosomal LINC01213 expression timing and CRPC progression?

In the proposed model for CRPC progression, we assume that each time-to-event variable (such as PSA progression and LINC01213-related transition time) follows a Weibull distribution, which is commonly used in biomedical studies for time-dependent outcomes. The initial assumption of independence between parameters is only for ease during model estimation; the joint likelihood function of the BBWD explicitly captures the dependency between both variables. This structure is similar to approaches used in recent biomedical models, such as those in recurrent event models using reflected Brownian motion, which handle patient-level variability, or cure models that link survival outcomes with biomarker changes over time<sup>36</sup>. Like these models, BBWD handles uncertainty and variability in disease progression data. The assumption about error distribution follows typical conventions in survival analysis, where variation in biological responses over time is modeled stochastically.

#### Model validation and sensitivity analysis

Model adequacy was evaluated by assessing the goodness-of-fit between the observed data and the BBWD cumulative distribution function (CDF) and probability density function (PDF) using established statistical tests. Additionally, a comprehensive sensitivity analysis was performed by perturbing each parameter within biologically plausible intervals, quantifying the impact on joint survival probabilities and hazard rates.

The BBWD model fitted well with the observed joint distribution of biomarker dynamics and clinical progression times. It did a good job of capturing the random branching behaviour that is at the heart of CRPC pathophysiology. While direct experimental validation was not performed within this study, the parameter estimation grounded in rigorously collected clinical datasets, combined with robust statistical inference and sensitivity testing, supports the mathematical and biological likelihood of the BBWD model as a tool for modelling CRPC progression mediated by exosomal LINC01213.

### Data source and experimental context

The only secondary data used in this study comes from Guo et al.'s<sup>16</sup> publicly available dataset, which has results from experiments using LNCaP and PC-3 prostate cancer cell lines in co-culture assays. The authors performed no new biological or experimental procedures. The data used include expression levels of exosomal LINC01213 and clinical parameters related to CRPC progression.

The original study provides detailed information on experimental design, including the use of control groups, co-culture conditions, and replicate counts. These conditions were preserved during data extraction and informed the statistical modelling and parameter estimation processes presented here. This study focuses solely on the development and application of a novel statistical model, the BBWD, to analyse these published data.

To enhance reproducibility, this study emphasizes complete transparency in the computational methods used to implement the BBWD model for CRPC. The analysis relies on secondary data obtained from previously published experimental studies. The workflow involved (1) collecting data from existing biomedical literature, (2) performing distribution analysis to identify the appropriate statistical model, (3) fitting mathematical models and verifying their suitability, (4) determining BBWD as the best-fit model for the data, and (5) interpreting the results based on the fitted model and collected data.

## Results

### The mathematical part of the biological medical system (effects of exosomes in the presence of prostate cancer through ADT)

Synchronization of the biomedical part into mathematical modelling follows:

In this study, biological experiments involving the co-culturing of LNCaP cells with PC-3 cells, PC-3 exosomes, and Si-LINC01213 were mathematically integrated into the Bayesian Belief Network with Data (BBWD) framework through the Joint Effect on Log-Likelihood Function (JELF). The JELF provides a comprehensive likelihood-based measure that captures the joint behaviour of paired observations under different experimental conditions. From (2), we can present a JELF for LNCaP, which was co-cultured with various cells, such as PC-3, PC-3 exosomes, and Si-LINC01213, to investigate the cell growth of the above-mentioned cells in combination with LNCaP in both normal and androgen-deprived medium.

For the normal medium, the JELF is defined as:

$$JELF(\alpha) = \sum_{k_1=1}^5 \ln f_1(x_1, x_2) + \sum_{k_2=1}^5 \ln f_2(y_1, y_2) + \sum_{k_3=1}^5 \ln f_3(z_1, z_2) \quad (3)$$

Here,

- $f_1(x_1, x_2)$  models the joint distribution of LNCaP cells co-cultured with PC-3 cells,
- $f_2(y_1, y_2)$  indicates PC-3 exosome cells in LNCaP,
- $f_3(z_1, z_2)$  indicates Si-LINC01213 cells in LNCaP, and  $\alpha$  denotes the normal medium of castration.

This formulation effectively aggregates the log-likelihoods from these three related but distinct biological interactions. Maximizing  $JELF(\alpha)$  allows estimation of parameters that best fit the observed cell growth and biomarker behaviour in the normal medium.

Similarly, for the androgen-deprived medium, the JELF is:

$$JELF(\beta) = \sum_{k_1=1}^5 \ln g_1(x_1, x_2) + \sum_{k_2=1}^5 \ln g_2(y_1, y_2) + \sum_{k_3=1}^5 \ln g_3(z_1, z_2) \quad (4)$$

where,

- $g_1, g_2, g_3$  correspond to the same biological pairs as above but under androgen deprivation
- $\beta$  represents the parameter set specific to the androgen-deprived medium.

### Consolidation and overview of results

LNCaP cells co-cultured with PC-3 cells in an androgen-deprived medium have much better results, with a little upliftment on the 5th day after a hike on day 4. Still, in normal medium, this combination is nevertheless found useful for the first two days and reaches its peak on the 5th day (Fig. 1a,b). When exosomes are added to the above combination in a normal medium, the combination produces a monotonically increasing curve that peaks on day four and neutralizes on day five. However, the combination in an androgen-deprived medium produces a similar monotonically increasing curve with a better magnitude on the Y-axis. In contrast, the normal medium produces a chaotic curve that ends close to the very lower amount of castration (Fig. 1c,d).



Si-LINC01213-1 has little forward result in the normal medium, whereas SiLINC01213-2 is chaotic. Our breakthrough is that LINC01213-1 and LINC01213-2 in the androgen-deprived medium yield significantly better results in castration compared with all the remaining treatment techniques. For the second day, the effects of LINC01213-1 and LINC01213-2 merged; on the 3<sup>rd</sup> and 4<sup>th</sup> days, LINC01213-2 reached minimum mode, while LINC01213-1 remained neutral. Surprisingly, LINC01213-2 has suddenly become unstable (Fig. 1e,f).

Simultaneously, LINC01213-1 stabilises on the 5th day with a lesser effect than LINC01213-2. Therefore, we concur with the medical statement that LINC01213 may be a novel therapeutic target for patients with CRPC. We are providing clarification and a detailed report for the treatment technique given to androgen-dependent prostate cancer-affected patients, and leading the final statement that exosomal LINC01213 plays an unavoidable pivotal role in the androgen-dependent prostate cancer cells, leading to androgen-independent behaviour.

Our recently developed mathematical modelling demonstrates that co-culturing LNCaP with PC-3 cells decreases the complexity of cell curation. Surprisingly, the model also shows how healthy cells can grow in a medium lacking androgens, with the help of fewer PC-3 exosomes interacting with LNCaP cells after they have multiplied (Fig. 2). We used the BBWD to determine how LNCaP cells changed over five days before and after they were co-cultured with PC-3 cells. Initially, the BBWD values for LNCaP cells were 1.5 on day 1, 0.35 on day 2, 0.67 on day 3, 0.35 on day 4, and 0.16 on day 5. After co-culturing with PC-3 cells, the BBWD values decreased to 1.03 on day 1, 0.29 on day 2, 0.28 on day 3, 0.14 on day 4, and 0.12 on day 5, indicating a significant decrease in the affected LNCaP cells.

Similarly, BBWD values for LNCaP cells with PBS over five days were initially 0.86 on day 1, 1.7 on day 2, 1.93 on day 3, 2.1 on day 4, and 1.79 on day 5. After co-culturing with exosomes, these values changed significantly to 1.98 on day 1, 1.56 on day 2, 0.68 on day 3, 1.33 on day 4, and 0.3 on day 5. These results illustrate a notable decrease in affected LNCaP cells over the five days following exosome co-culturing. Overall, the BBWD model effectively highlights the impact of co-culturing on cell behaviour and viability, demonstrating a significant reduction in affected cells.

## Discussion

### An overview of the biological medical system

As per the medical treatment analysis of prostate cancer, the development of this kind of cancer is complex by nature. The transition from androgen-dependent to androgen-independent is considered more complex by nature. Androgen-dependent prostate cancer (ADPC) cells and androgen-independent prostate cancer (AIPC) cells can coexist for a specific period. Henceforth, the vital role of exosomes is confirmed in this transformation.

Even non-coding RNAs in exosomes are crucial in many cancers; however, CRPC exosomes have not been reported. Zhuifeng Guo et al. found that cell co-culture elevated LINC01213, demonstrating exosomes' participation in CRPC. Co-cultured LNCaP and PC-3 cancer cells demonstrate that the androgen-deprived group had more LNCaP cells than the normal group. Exosomes were suspected in PC-3 cells due to exosomal granules. LNCaP co-culture with PC-3 resulted in separated exosomes from PC-3, which reduced AR and PSA levels as determined by Western blotting.

To make AIPC cells less likely to be emasculated, PC-3 exosomes were co-cultured with LNCaP cells to determine if they would proliferate. They did, and the cells multiplied more in a medium that lacked androgens. MicroRNA, lncRNA, and circRNA are common exosome components. Instead, lncRNA was used to explore the mechanisms of exosomes' castration resistance. LINC01213 stimulation in prostate cancer was examined for prognosis. This suggests that LINC01213 minimises ADPC cell androgen dependence.

### Statements derived from the bio-system

The results support our study's hypothesis, which states that growing PC-3 cells with LNCaP cells in an androgen-rich medium can stimulate LNCaP cell proliferation. However, it is yet unknown how PC-3 cells confer castration resistance on LNCaP cells.

Exosomes function both in vivo and in vitro. The findings significantly improved the terminology of LNCaP cells following treatment with PC-3 exosomes. Under culture settings, normal LNCaP cells could not proliferate; however, after being treated with PC-3 exosomes, the cells developed tumors. In other words, exosomes play a crucial role in the transformation process.

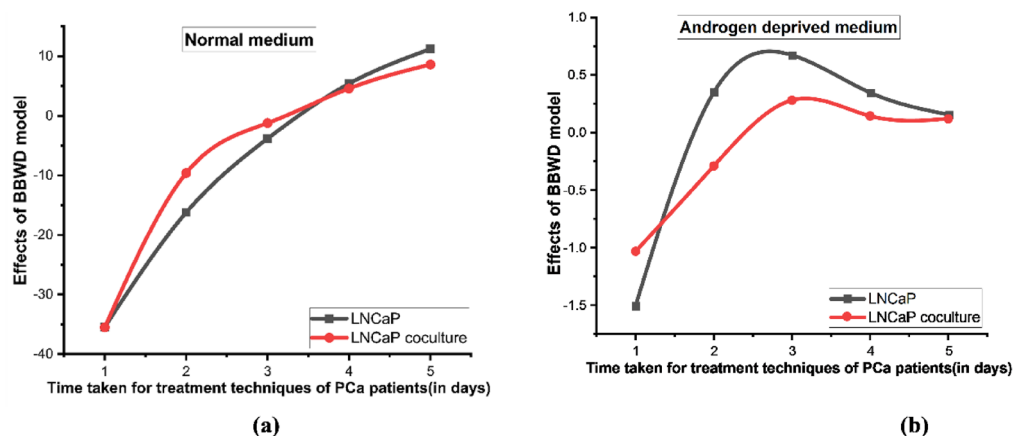
Overall, the biosystem demonstrates for the first time that LINC01213 molecules are present in the exosomes of prostate cancer cells. Furthermore, the author speculates that their research could offer fresh approaches to treating CRPC by categorising the function of the tumour microenvironment in the disease's development<sup>16</sup>.

### Prostate cancer therapy methods comprise the bio system

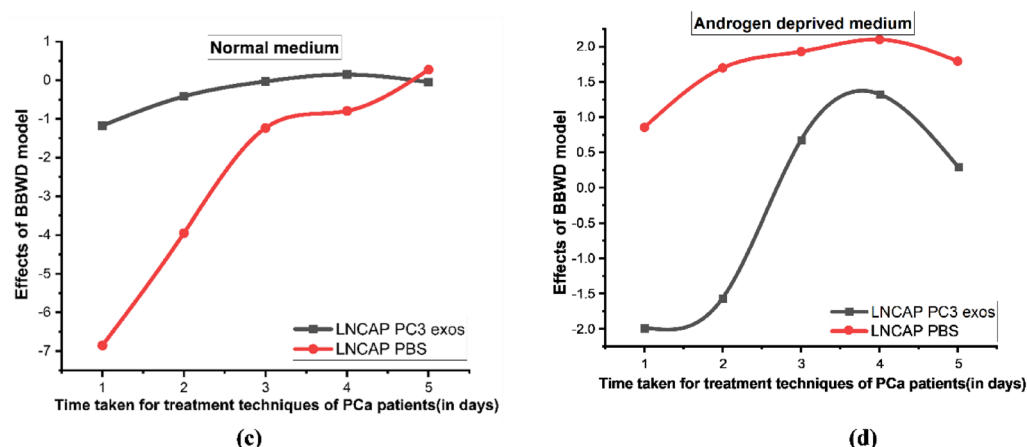
The following steps have been done to analyse the impact of exosomes LINC01213 in androgen-deprived prostate cancer in a biological system.

- **Step 1:** LNCaP cells and PC3 cells were co-cultured in a transwell system (Fig. 3).
- **Step 2:** Exosomes were separated from PC-3 because they were thought to be PC-3 exosomes. Western blotting was used to identify the features of the exosomes (Fig. 4).
- **Step 3:** To prevent emasculation, AIPC cells generate exosomes that activate ADPC cells. This causes an increase in LNCaP cells in both general and androgen-deficient conditions.
- **Step 4:** Although exosomes include a variety of substances, lncRNA was concentrated to examine LINC01213, which has been linked to prostate cancer.
- **Step 5:** The preformation of LNCaP cells was to occur under normal circumstances by the preceding procedure, and they are unable to multiply in the absence of androgen, which demonstrated that in LNCaP cells, downregulating LINC01213 reduced the amounts of  $\beta$ -catenin protein (Fig. 5).

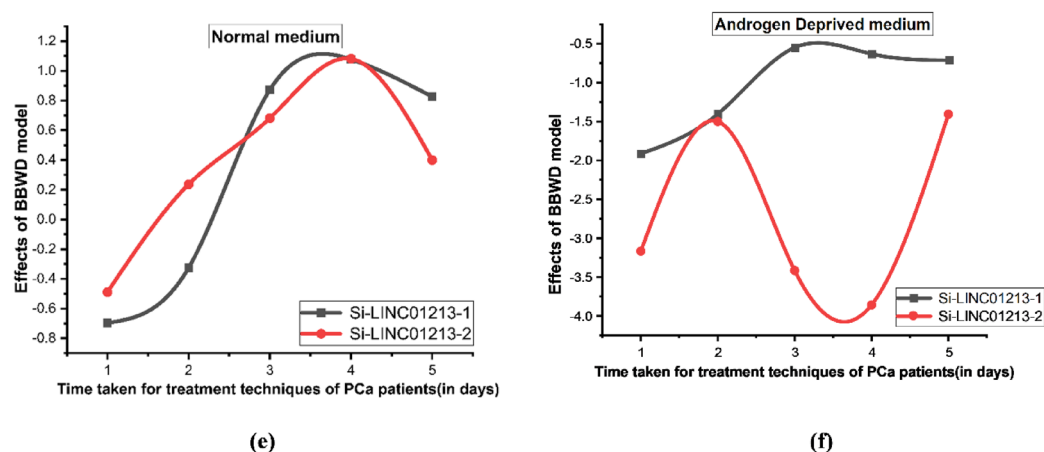
### 1.1 BBWD Modelling response of LNCaP cells with and without PC-3 co-culture



### 1.2 BBWD Modeling of LNCaP Treated with PC-3 Exosomes



### 1.3 BBWD Modelling for effects of LINC01213 reduced (Si-LINC01213-1 and Si-LINC01213-2) on LNCaP cells



The above results have been classified using our mathematical model, specifically the branching bivariate Weibull distribution, which yields the following for each type of proliferation.

- Normal medium:** Effects of LNCaP cells with PC-3 cells in the normal medium are nevertheless useful, and for the first two days, it has negative results that are neutralised on the 3rd day but rise on the 4th day and reach maximum mode on the 5th day (Fig. 1a).

**Fig. 1.** BBWD modelling of LNCaP cell responses under various treatments and culture conditions: (a) In normal medium, LNCaP co-cultured with PC-3 shows faster recovery than LNCaP alone. (b) In androgen-deprived medium, co-cultured LNCaP exhibits more stable performance, indicating improved androgen-independent behaviour. (c) In normal medium, LNCaP cells treated with PC-3 exosomes maintain near-stable, while PBS-treated controls show progressive improvement over five days. (d) In androgen-deprived medium, exosome-treated LNCaP cells exhibit fluctuation, whereas PBS-treated cells show gradual but steady effects, suggesting distinct stress adaptation profiles. (e) In normal medium, both siRNA treatments show similar trends with slight differences in peak response and decline. (f) In androgen-deprived medium, Si-LINC01213-2 shows a more variable response compared to the steady profile of Si-LINC01213-1, suggesting differing roles in androgen-independent adaptation.

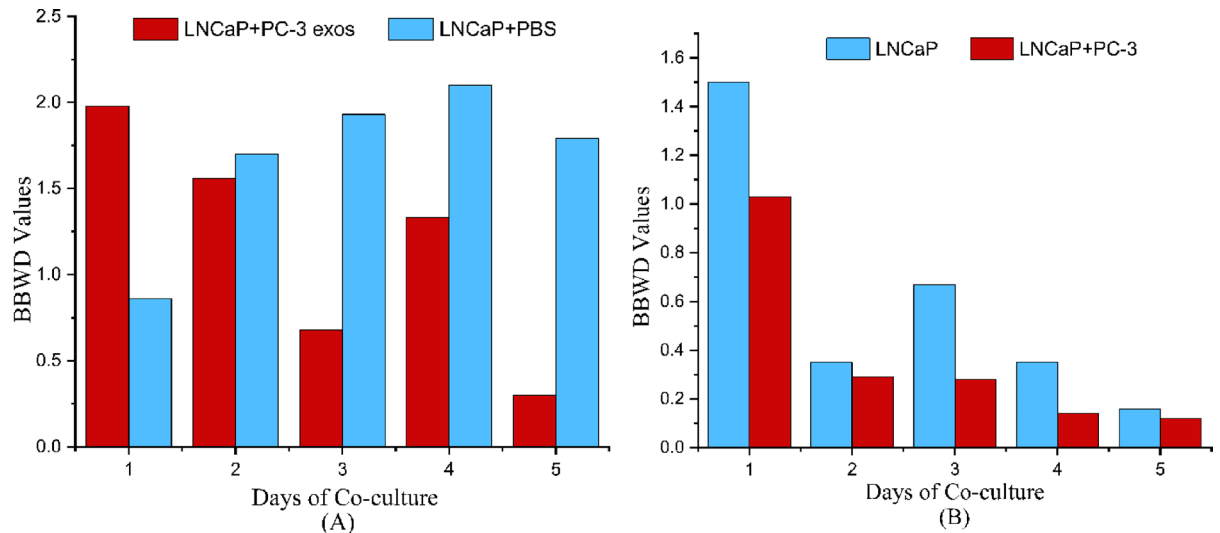


**Fig. 2.** BBWD analysis of LNCaP cells under different co-culture conditions with PC-3 cells over five days. (A) LNCaP cells were treated with PC-3-derived exosomes compared to PBS-treated controls. The results show a progressive reduction in BBWD values in the exosome-treated group, indicating a decrease in affected cell populations. (B) LNCaP cells before and after direct co-culture with PC-3 cells. A notable decrease in post co-culture suggests reduced cell complexity and enhanced viability in androgen-deficient conditions due to interaction with PC-3 cells.

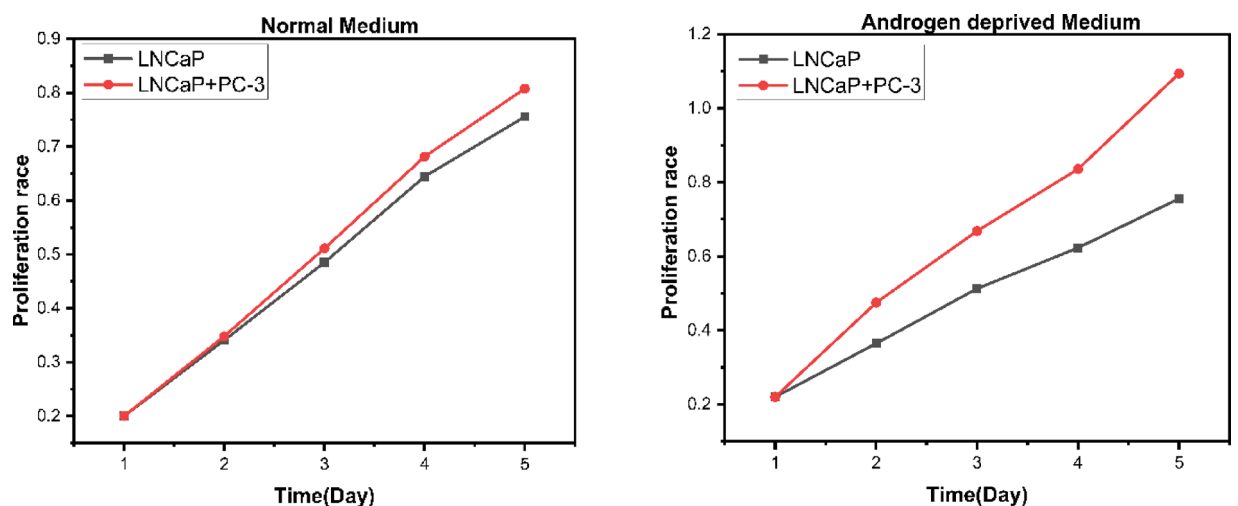


**Fig. 3.** Variation in resistance of LNCaP cells in co-culture with PC-3 cells: Depicting the proliferation of LNCaP and PC-3 cells in both normal and androgen-deprived medium<sup>16</sup>.

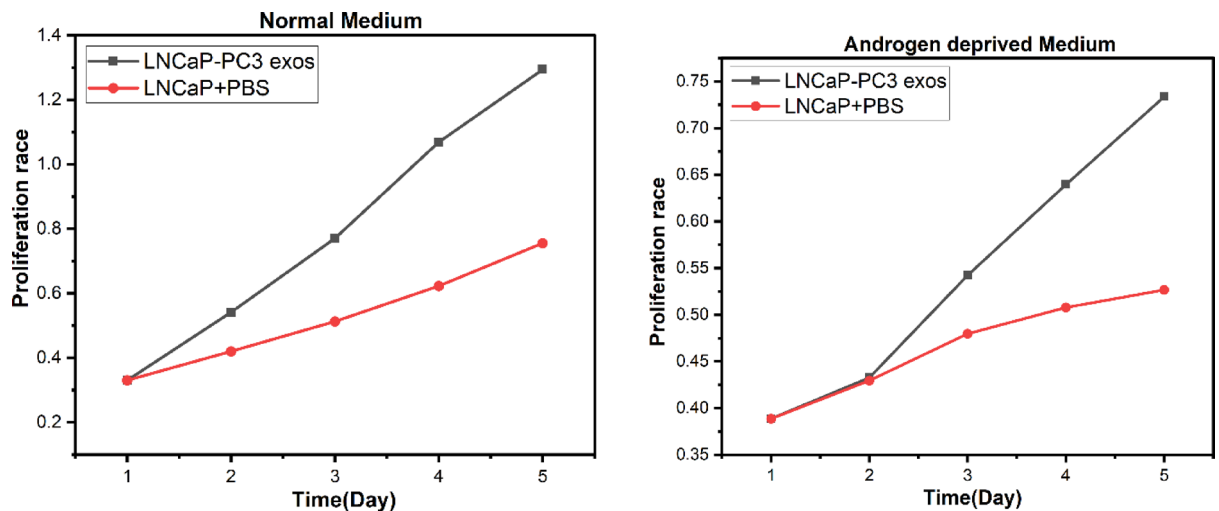


**Fig. 4.** Role of PC-3-derived exosomes in the development of castration resistance in LNCaP cells: Proliferation of LNCaP and PC-3 cells treated with exosomes, assessed in both normal and androgen-deprived medium<sup>16</sup>.

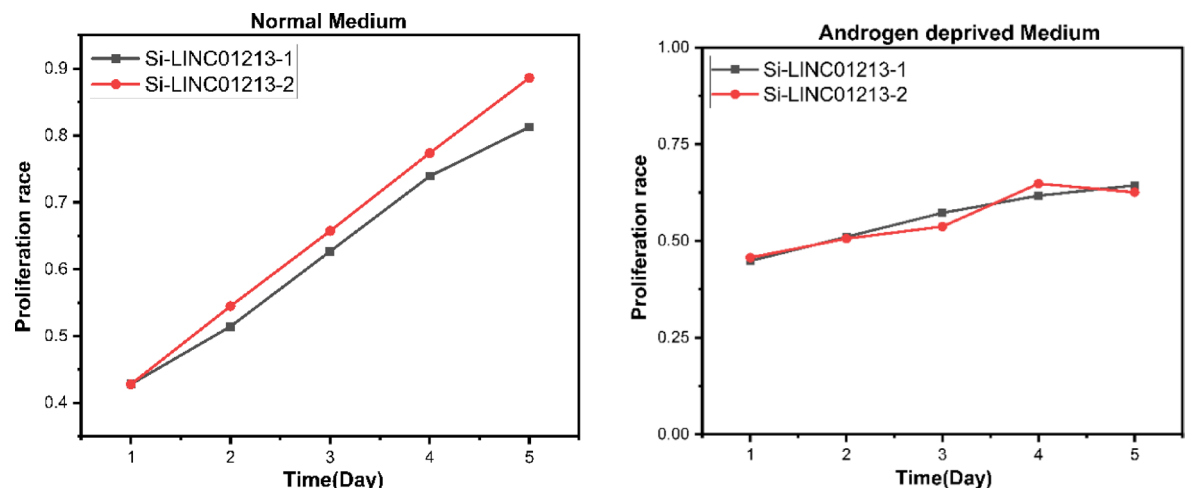


**Fig. 5.** LINC01213 promotes androgen-independent behaviour through Wnt/β-catenin signalling: Cell proliferation of si-LINC01213-1 and si-LINC01213-2 transfected LNCaP cells in both normal and androgen-deprived medium<sup>16</sup>.

- *Androgen-deprived medium:* Effects of LNCaP cells with PC-3 cells in androgen-deprived medium have much better results than in normal medium; that is, LNCaP with PC-3 cells were raised on the 2nd day, and little upliftment was neutralised on the 5th day after a hike on the 4th day (Fig. 1b).
- *Normal medium:* When LNCaP and PC-3 cells are treated with exosomes in normal medium, the effect of LNCaP with PC-3 exosomes is far away from LNCaP on the very first day and is nearing on the 3rd and 4th days but is synchronised on the 5th day of castration (Fig. 1c).
- *Androgen-deprived medium:* There is no synchronisation in an androgen-deprived medium between LNCaP with PC-3 exosomes and LNCaP, whereas LNCaP with PC-3 exosomes has decreased markedly, which indicates that there is an ability to form a tumour (Fig. 1d).
- In order to identify the resistance to castration for androgen-independent prostate cancer exosomes, the effect of lncRNA in LNCaP cells was tested using RNA sequencing before and after the treatment of PC-3 exosomes. Therefore, an extended intergenic non-coding RNA, specifically LINC01213, was found to be upregulated through the β-catenin pathway. Thus, the mathematical result follows for the process mentioned above.
- *Normal medium:* Si-LINC01213-2 cell growth was raised evenly for the first three days and synchronised with Si-LINC01213-1 on the 4th day, reducing on the 5th day (Fig. 1e).
- *Androgen-deprived medium:* The cells Si-LINC01213-1 and Si-LINC01213-2 overlapped for the second day, and the distance between them was increased on the 4th day, then suddenly reduced on the 5th day (Fig. 1f).

## Implications of the study

The research has significant implications for statistical modelling and clinical oncology, treating CRPC. It shows the BBWD model, which helps us learn a lot more about how androgen-dependent prostate cancer changes into androgen-independent prostate cancer and how this changes the survival and failure rates of CRPC treatments. This model fills a crucial gap in evaluating therapeutic efficacy, particularly in androgen-deprived environments where traditional models fail to capture the complexities of CRPC progression.

- *New analytical framework of CRPC:* The model offers a more sophisticated approach to evaluating the progression of androgen-dependent cancer to states independent of androgen influence. This refinement in prediction could be a beacon of hope, potentially leading to the development of personalized therapies for patients with CRPC.
- *Potential therapeutic target in exosomal LINC01213:* The kinetics of exosomal LINC01213 in an androgen-deprived environment and a normal environment identify it as a promising therapeutic target. This might be useful while guiding treatments that reduce reliance on androgen, as exosomal LINC01213 promotes the survival of cancer cells even under conditions with low androgen levels.
- *Better analysis of treatment effectiveness:* The BBWD model and the JELF will help you study different treatment methods by showing statistically that LINC01213 works well in media that don't have androgens. The medical fraternity and researchers will now have a novel tool to analyse how interventions in treatment affect cancer progression in different biological conditions.
- *Advancement in the statistical modeling of biomedicine:* This work contributes to the development of biostatistics by demonstrating how the BBWD distribution can be applied well after survival analysis. Bivariate models are emphasized in clinical research for complex diseases, where multiple biological pathways contribute to treatment outcomes.

This study's findings and methodological advances promise to be valuable for improving prostate cancer treatment strategies and statistical applications in medicine. They will present clinicians and researchers with a powerful tool to understand and potentially overcome the challenges CRPC poses, paving the way for more effective targeted therapies against cancer.

## Conclusions

A medicinal biosystem consisting of the treatment technique given for the transition of androgen-dependent prostate cancer into androgen-independent behaviour is taken into account. The proposed branching bivariate Weibull distribution (BBWD) model seeks to determine the optimal solution for the bio variable and draw conclusions for the medical field. Our breakthrough is that the kinetics of LINC01213 in the androgen-deprived medium yield significantly better results in castration compared with all the remaining treatment techniques. The results derived from the BBWD model suggest that the statements obtained by the medical system are veracious. As a result, we agree with the medical part that LINC01213 may be a new therapeutic target for CRPC patients. We are also giving more information about the treatment method used on patients with prostate cancer, which leads to the conclusion that Exosomal LINC01213 plays an essential role in the androgen-dependent prostate. Moreover, the joint effect on log-likelihood function (JELF) is an analytical barrier for the joint effect of LINC01213 both in normal and androgen-deprived mediums.

## Limitations

The study, while innovative, faces certain limitations. The BBWD model relies on mathematical estimations that may not fully capture the biological complexity of CRPC due to individual variations in patient responses. The model also relies on MLE and JELF, which are assumed to exhibit consistent parameter behaviours across patient samples, whereas genetic and environmental differences might influence the course of CRPC.

While the present study provides a novel statistical analysis of exosomal LINC01213 using the BBWD model, it is based entirely on secondary data from previously published experiments. While this study highlights the role of exosomal LINC01213 in CRPC progression, focusing exclusively on this biomarker limits the scope of the findings. Other molecular factors and pathways likely contribute to the disease's complexity and may interact with LINC01213, but were not considered in this study. Additionally, the reliance on secondary data and statistical modelling means that biological validation and experimental confirmation are still needed.

To enhance the clinical relevance and therapeutic robustness of the model, future work should involve prospective validation using experimental co-culture studies or clinical sample analysis. Additionally, applying the model to larger and more diverse biological datasets could help confirm its applicability and strengthen its predictive value in real-world settings.

## Future directions

Potential areas for future work from this study include extending the BBWD model to include more biomarkers and molecular pathways beyond exosomal LINC01213, thereby further elucidating the complex dynamics in CRPC. In this way, the integration of genomic and proteomic data may enrich the model to enable predictions that consider patient variability. To make it more valuable and reliable for CRPC populations, it will be essential to conduct further testing with extensive clinical data and diverse patient groups. Future research should integrate multiple biomarkers and combine computational models with prospective experimental or clinical studies. Expanding the dataset and incorporating dynamic biological interactions will improve model accuracy and enhance personalised therapeutic insights for CRPC.

To make it more useful in oncology as a whole, it may also be helpful to explore how BBWD can be applied to evaluate other or similar cancers or treatments that rely on androgen-related dynamics. Adopting this model



for the real-time analysis of patients' response to CRPCs can be positive for deriving tailored therapeutic interventions that may improve more accurate and targeted treatment in cancer care.

## Data availability

All data generated or analyzed during this study are included in this published article.

Received: 1 November 2024; Accepted: 16 June 2025

Published online: 08 July 2025

## References

- Chen, J., Zhang, D., Yan, W., Yang, D. & Shen, B. Translational bioinformatics for diagnostic and prognostic prediction of prostate cancer in the next-generation sequencing era. *Biomed. Res. Int.* **2013**, 901578. <https://doi.org/10.1155/2013/901578> (2013).
- Dad, H. & Hansen, A. Advancements in research on non-AR-signaling pathways and targeted therapies for castration-resistant prostate cancer. *Ann. Urol. Oncol.* **8**(1), 12–20. <https://doi.org/10.32948/auo.2024.12.25> (2024).
- Hjelmberg, J. B. et al. The heritability of prostate cancer in the Nordic Twin Study of Cancer. *Cancer Epidemiol. Biomark. Prev.* **23**, 2303–2310. <https://doi.org/10.1158/1055-9965.EPI-13-0568> (2014).
- Zhou, Y. et al. Evaluation of urinary metal concentrations and sperm DNA damage in infertile men from an infertility clinic. *Environ. Toxicol. Pharmacol.* **45**, 68–73. <https://doi.org/10.1016/j.etap.2016.05.020> (2016).
- Gao, Y. et al. The effects and molecular mechanism of heat stress on spermatogenesis and the mitigation measures. *Syst. Biol. Reprod. Med.* **68**(5–6), 331–347. <https://doi.org/10.1080/19396368.2022.2074325> (2022).
- Bluemn, E. G. & Nelson, P. S. The androgen/androgen receptor axis in prostate cancer. *Curr. Opin. Oncol.* **24**, 251–257. <https://doi.org/10.1097/CCO.0b013e32835105b3> (2012).
- Li, K. et al. Advances in prostate cancer biomarkers and probes. *Cyborg. Bionic Syst.* **5**, 0129. <https://doi.org/10.34133/cbsystems.0129> (2024).
- Takayama, K. Splicing factors have an essential role in prostate cancer progression and androgen receptor signaling. *Biomolecules* **9**, 131. <https://doi.org/10.3390/biom9040131> (2019).
- Wang, K. et al. Extracellular matrix stiffness regulates colorectal cancer progression via HSF4. *J. Exp. Clin. Cancer Res.* **44**(1), 30. <https://doi.org/10.1186/s13046-025-03297-8> (2025).
- Simons, M. & Raposo, G. Exosomes–vesicular carriers for intercellular communication. *Curr. Opin. Cell Biol.* **21**, 575–581. <https://doi.org/10.1016/j.ccb.2009.03.007> (2009).
- Luan, F., Cui, Y., Huang, R., Yang, Z. & Qiao, S. Comprehensive pan-cancer analysis reveals NTN1 as an immune infiltrate risk factor and its potential prognostic value in SKCM. *Sci. Rep.* **15**(1), 3223. <https://doi.org/10.1038/s41598-025-85444-x> (2025).
- Li, Y. et al. Current landscape of exosomal non-coding RNAs in prostate cancer: Modulators and biomarkers. *Non-coding RNA Res.* <https://doi.org/10.1016/j.ncrna.2024.07.003> (2024).
- Wang, C. et al. Mesenchymal stromal cell exosomes for drug delivery of prostate cancer treatments: A review. *Stem Cell Res. Ther.* **16**, 18. <https://doi.org/10.1186/s13287-025-04133-8> (2025).
- El-Sherpieny, E. A., Muhammed, H. Z. & Almetwally, E. M. FGM bivariate Weibull distribution. In *Proceedings of the Annual Conference in Statistics (53rd), Computer Science, and Operations Research* vol. 55. (Institute of Statistical Studies and Research, Cairo University, 2018).
- He, B. et al. A fusion model to predict the survival of colorectal cancer based on histopathological image and gene mutation. *Sci. Rep.* **15**(1), 9677. <https://doi.org/10.1038/s41598-025-91420-2> (2025).
- Guo, Z. et al. Exosomal LINC01213 plays a role in the transition of androgen-dependent prostate cancer cells into androgen-independent manners. *J. Oncol.* **2022**, 8058770. <https://doi.org/10.1155/2022/8058770> (2022).
- Lu, J. C. & Bhattacharyya, G. K. Some new constructions of bivariate Weibull models. *Ann. Inst. Stat. Math.* **42**, 543–559. <https://doi.org/10.1007/BF00049307> (1990).
- Johnson, R. A. & Omori, Y. Influence of random effects on bivariate and trivariate survival models. *J. Nonparametr. Stat.* **11**, 137–159. <https://doi.org/10.1080/10485259908832778> (1999).
- Bosson-Amedeu, S., Ayitey, E. & Anafo, A. Y. *Mathematical Approaches to Understanding Prostate Cancer Progression: A Compartmental Modeling Study in Ghana*. <https://doi.org/10.21203/rs.3.rs-5282657/v1> (2024).
- Oakes, D. Multivariate survival distributions. *J. Nonparametr. Stat.* **3**, 343–354. <https://doi.org/10.1080/10485259408832593> (1994).
- Sahu, S. K., Dey, D. K., Aslanidou, H. & Sinha, D. A Weibull regression model with gamma frailties for multivariate survival data. *Lifetime Data Anal.* **3**, 123–137. <https://doi.org/10.1023/A:1009605117713> (1997).
- Mondal, S. & Kundu, D. A bivariate inverse Weibull distribution and its application in complementary risks model. *J. Appl. Stat.* **47**, 1084–1108. <https://doi.org/10.1080/02664763.2019.1669542> (2020).
- Gupta, R. D. & Kundu, D. A new class of weighted exponential distributions. *Statistics (Berl.)* **43**, 621–634. <https://doi.org/10.1080/02331880802605346> (2009).
- Ettoumi, F. Y., Sauvageot, H. & Adane, A.-E.-H. Statistical bivariate modelling of wind using first-order Markov chain and Weibull distribution. *Renew. Energy* **28**, 1787–1802. [https://doi.org/10.1016/S0960-1481\(03\)00019-3](https://doi.org/10.1016/S0960-1481(03)00019-3) (2003).
- Kundu, D. & Gupta, A. K. On bivariate Weibull-geometric distribution. *J. Multivar. Anal.* **123**, 19–29. <https://doi.org/10.1016/j.jmva.2013.08.004> (2014).
- Hanagal, D. D. Frailty regression models in mixture distributions. *J. Stat. Plan. Inference* **138**, 2462–2468. <https://doi.org/10.1016/j.jspi.2007.10.014> (2008).
- Lakshmi, S. & Gayathri, M. Mathematical model for the secretion of oxytocin after vaginal delivery or caesarean in breastfeeding women. *Int. J. Engin. Res. Appl.* **4**, 19–24 (2014).
- Lakshmi, S. & Goperundevi, M. A mathematical model for the genetic variation of prolactin and prolactin receptor in relationship with serum prolactin concentrations and breast cancer risk. *Int. J. Eng. Res. Appl.* **4**, 12–18 (2014).
- Lakshmi, S. & Manickam, A. A mathematical Weibull model for blunted growth hormone response to maximal exercise in middle-aged versus young subjects and no effect of endurance training. *Elderly* **3**, 6 (2014).
- Lakshmi, S. & Manickam, A. A stochastic process degradation model for effects of 3-year GH replacement therapy for GH deficiency on bone mineral density in younger and elderly adults. *J. Adv. Math.* **7**, 2 (2014).
- Ignatia, M. J. & Lakshmi, S. Mathematical model for finding the bounds of Estrone sulfate by using Estrone and Estradiol. *Int. J. Appl. Math. Sci.* **6**, 19–27 (2013).
- Ignatia, M. J. & Lakshmi, S. Stochastic modeling for the secretion of Estrogen by using total time on test transform. *Am. J. Math. Math. Sci.* **2**, 165–172 (2013).
- Ignatia, M. J. & Lakshmi, S. Mathematical degradation model for transcriptional regulation of BRCA1. *Int. J. Latest Trends Eng. Technol.* **8**, 440–448 (2017).
- Ignatia, M. J. & Lakshmi, S. Mathematical model for the stress effect of estrogen on bone mineral density in case of osteoporosis. *Int. J. Recent Innov. Trends Comput. Commun.* (2020).



35. Ignatia, M. J. & Lakshmi, S. A trivariate Weibull model of effects of Drospirenone and Estrogen in postmenopausal women with hypertension. *Int. J. Appl. Eng. Res.* **13**, 6628–6635 (2018).
36. Enoyoze, E. & Enoyoze, G. E. Statistical applications in the biomedical sciences: A review. *Int. J. Sci. Res. Arch.* **12**, 1594–1601. <https://doi.org/10.30574/ijrsra.2024.12.2.1433> (2024).

## Author contributions

Conceptualization, M.S., K.M.J.I., M.J.D.; methodology, R.K., A.K.B.; software, M.S., K.M.J.I., M.J.D., R.K., A.K.B.; validation, M.S., K.M.J.I., H.K.C., A.B., J.L.; formal analysis, M.S., K.M.J.I., M.J.D., R.K., A.K.B., J.L.; investigation, M.S., A.B., J.L.; resources, H.K.C., A.B., J.L.; data curation, M.S., K.M.J.I., M.J.D.; writing—original draft preparation, M.S., K.M.J.I., M.J.D., R.K.; writing—review and editing, M.S., K.M.J.I., M.J.D., R.K., A.K.B., R.S., H.K.C., A.B., J.L.; visualization, A.K.B., R.S.; supervision, R.K., A.K.B., R.S., H.K.C.; project administration, R.S., H.K.C., A.B., J.L.; funding acquisition, J.L.

## Declarations

### Competing interests

The authors declare no competing interests.

### Additional information

**Correspondence** and requests for materials should be addressed to J.L.

**Reprints and permissions information** is available at [www.nature.com/reprints](http://www.nature.com/reprints).

**Publisher's note** Springer Nature remains neutral with regard to jurisdictional claims in published maps and institutional affiliations.

**Open Access** This article is licensed under a Creative Commons Attribution-NonCommercial-NoDerivatives 4.0 International License, which permits any non-commercial use, sharing, distribution and reproduction in any medium or format, as long as you give appropriate credit to the original author(s) and the source, provide a link to the Creative Commons licence, and indicate if you modified the licensed material. You do not have permission under this licence to share adapted material derived from this article or parts of it. The images or other third party material in this article are included in the article's Creative Commons licence, unless indicated otherwise in a credit line to the material. If material is not included in the article's Creative Commons licence and your intended use is not permitted by statutory regulation or exceeds the permitted use, you will need to obtain permission directly from the copyright holder. To view a copy of this licence, visit <http://creativecommons.org/licenses/by-nc-nd/4.0/>.

© The Author(s) 2025